AFM Studies of the Molecular Weight Dependence of Lamellar Growth Kinetics of Polymers near the Glass Transition Temperature

Yong Wang,[†] Chi-Ming Chan,*[,†] Yong Jiang,[§] Lin Li,[§] and Kai-Mo Ng[†,‡]

Department of Chemical Engineering and Advanced Engineering Materials Facility, Hong Kong University of Science and Technology, Clear Water Bay, Kowloon, Hong Kong, and State Key Laboratory of Polymer Physics and Chemistry, Center for Molecular Science, Institute of Chemistry, Chinese Academy of Sciences, Beijing 100080, China

Received November 26, 2006; Revised Manuscript Received March 14, 2007

ABSTRACT: The dependence of the lamellar growth kinetics on the molecular weight (MW) of poly(bisphenol A octane ether) (BA-C8) in the low crystallization temperature region was investigated using atomic force microscopy (AFM). We found that Lauritzen−Hoffman's theory can be used to analyze kinetics data of BA-C8 samples obtained in regimes I and II but not regime III. A new expression of lamellar growth kinetics was proposed on the basis of a simple kinetic model with a rough surface.

1. Introduction

Molecular weight (MW) plays a vital role in governing the crystallization kinetics and morphology of polymers.[1] In past decades, the effects of MW on crystal growth kinetics have been the subject of various investigations.[2−15] Using optical microscopy (OM) to analyze spherulitic growth, Magill reported a decrease in the growth rate as the MW of poly(tetramethyl-*p*-silphenylenesiloxane) increased.[2−4] Similar results were obtained by Hoffman,[5] Hoffman and Miller,[1] and Cheng et al.[6] The MW dependence of the crystal growth rate at relatively high crystallization temperatures (small supercooling, $\Delta T = T_m^0 - T_c$, where T_m^0 is the equilibrium melting point and T_c is the crystallization temperature) was shown to follow a power law relationship between the growth rate and the molecular weight, MW^{α} (where α is a constant). Different values of α were reported by Magill et al.,[11] Hoffman and Miller,[1] and Hikosaka et al. [12,13] Magill showed that $\alpha = -0.5$ for the spherulitic growth of poly(tetramethyl-*p*-silphenylenesiloxane) and poly(ethylene terephthalate).[11] Hoffman and Miller studied the spherulites or axialites of polyethylene (PE) and found that α ranged from -1.3 to -1.8.[1] Hikosaka et al. measured the growth rate of single (or single-crystal-like) crystals of PE. They found that $\alpha = -1.7$ and -0.7 for folded chain single crystals and extended chain single crystals, respectively.[12,13]

The dependence of polymer crystallization kinetics on T_c and MW must be considered simultaneously. In general, a bell-shaped curve showing the crystallization rate as a function of T_c with a maximum value existing somewhere between T_g and T_m is obtained. In the low crystallization temperature region (near T_g), the crystal growth rate strongly depends on T_c; in the high crystallization temperature region (near T_m), the growth rate depends on ΔT. On the basis of the crystallization of highly crystallizable, flexible-chain polymers (e.g., PE), two main theories have been proposed, namely, the Lauritzen−Hoffman secondary nucleation (LH) theory[1,5,14] and Sadler's rough surface theory.[15−18]

Although the preceding works have advanced our understanding of the MW dependence of polymer crystallization kinetics, these studies focused mainly on the crystallization of polymers near T_m at the micron-scale level studied by OM. In crystallization near T_m, the motion of polymer chains is carried out entirely via molecular reptation,[14,19] while in crystallization near T_g, polymer chains complete their conformation rearrangement via cooperative segmental movements (i.e., segmental diffusion).[20] Only a few studies have been performed at temperatures near T_g at the lamellar level. As a result, many fundamental questions have remained unanswered. For example, what is the relationship between the MW and the growth rate of lamellae at crystallization temperatures near T_g? Does the dependence on MW differ at different T_cs? Does the well-known LH theory work in regime III?

In recent years, the study of crystallization kinetics and the morphology of polymers using atomic force microscopy (AFM) has become popular due to the ability of AFM to obtain in-situ and real-time structural information on the nanometer scale. In particular, tapping-mode AFM (TM-AFM) with the phase imaging function substantially complements OM with its high resolution and also complements transmission electron microscopy (TEM) because it can be used under ambient conditions for real-time observations and does not require special sample treatment. TM-AFM has been increasingly used to study the lamellar growth rate and the lamellar structures of various semicrystalline polymers.[21−35] Hobbs et al. studied the growth of lamellae and spherulites of poly(hydroxybutyrate-*co*-valerate) by TM-AFM equipped with a hot stage. They found that the growth rate of lamellae is different from the spherulitic growth rate and is not always constant. The former is usually larger than the latter.[29] Similar results were also obtained by Li et al. on poly(bisphenol A octane ether) (BA-C8) at room temperature.[30] In addition, Beekmans et al.,[32] Lei et al.,[33] and Jiang et al.[35] have also successfully determined the lamellar growth rates of polymers at various T_cs by hot-stage TM-AFM.

As we previously reported,[25,28,30,33−35] our real-time TM-AFM observations of the formation of spherulites of BA-C8 suggested that a spherulite starts with the birth of an embryo, which develops into a founding lamella. Through branching and splaying, the founding lamella grows into a lamellar sheaf and then finally forms a mature spherulite. Moreover, in the initial

* To whom correspondence should be addressed.
[†] Department of Chemical Engineering, Hong Kong University of Science and Technology.
[‡] Advanced Engineering Materials Facility, Hong Kong University of Science and Technology.
[§] Chinese Academy of Sciences.

10.1021/ma062717y CCC: $37.00
Published on Web 05/04/2007

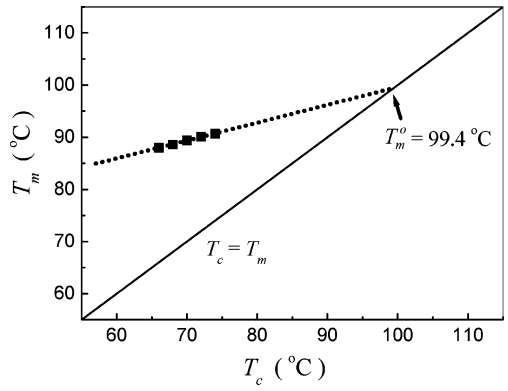

Figure 1. Hoffman−Weeks plot to determine the T_m^0 of a BA-C8 sample (S-3).

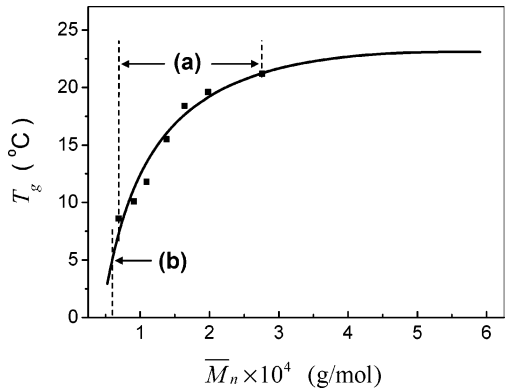

Figure 2. Plot of T_g as a function of $\bar{M}_n$ of BA-C8 samples. Label a indicates the $\bar{M}_n$ range of the BA-C8 samples used in this study; label b is the $\bar{M}_c$ (about 6000 g/mol) for BA-C8.

Table 1. Molecular Characteristics of BA-C8 Samples

sample	$\bar{M}_n$ [g/mol]	$\bar{M}_w$ [g/mol]	$\bar{M}_w/\bar{M}_n$	T_g (°C)	T_m^0 (°C)
S-1	27 600	35 900	1.30	21.2	102.3
S-2	19 800	28 200	1.42	19.6	101.5
S-3	16 400	25 000	1.52	18.4	99.4
S-4	13 800	21 200	1.54	15.5	98.3
S-5	10 900	17 000	1.56	11.8	98.1
S-6	9 100	14 400	1.58	10.1	95.4
S-7	6 900	12 600	1.83	8.6	94.2

and middle stages of the formation of spherulites (before the impingement of spherulites occurs), the average growth rates of all lamellae that grow outward radially on the fringe of a spherulite are almost uniform.

In this paper, the MW dependence of lamellar growth kinetics was studied at various temperatures. The lamellar growth rates of the BA-C8 samples at different T_cs were measured, and the results, showing the presence of regimes I and II, agreed with that predicted by the LH crystallization theory. However, at different T_cs (regime III), the data did not fit well with that predicted by the LH crystallization theory. A new expression of lamellar growth kinetics is proposed here on the basis of a simple kinetic model of the attachment of chain segments to crystal growing surfaces during crystallization.

2. Experimental Section

BA-C8 was synthesized by condensation polymerization of bisphenol A and 1,8-dibromooctane.[25] The MWs of the BA-C8 samples were controlled by a stiochiometric imbalance between bisphenol A and 1,8-dibromooctane. A slightly excessive amount of 1,8-dibromooctane was used to ensure that the Br was the end group. With the same amount of catalyst and the same reaction time, a larger stiochiometric imbalance resulted in a lower molecular

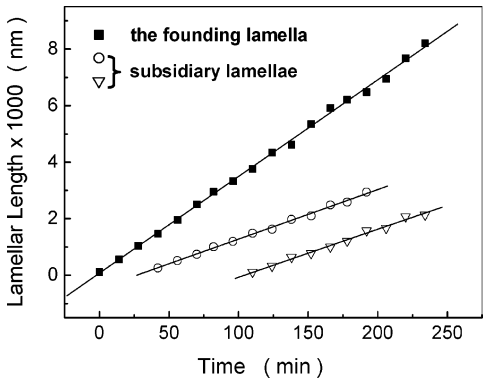

Figure 3. Plot of lamellar length vs time. The measurements were made on one spherulite of a BA-C8 sample (S-5). The slope values of the fitting lines of a founding lamella and two subsidiary lamellae are 34.2, 17.5, and 16.9 nm/min, respectively.

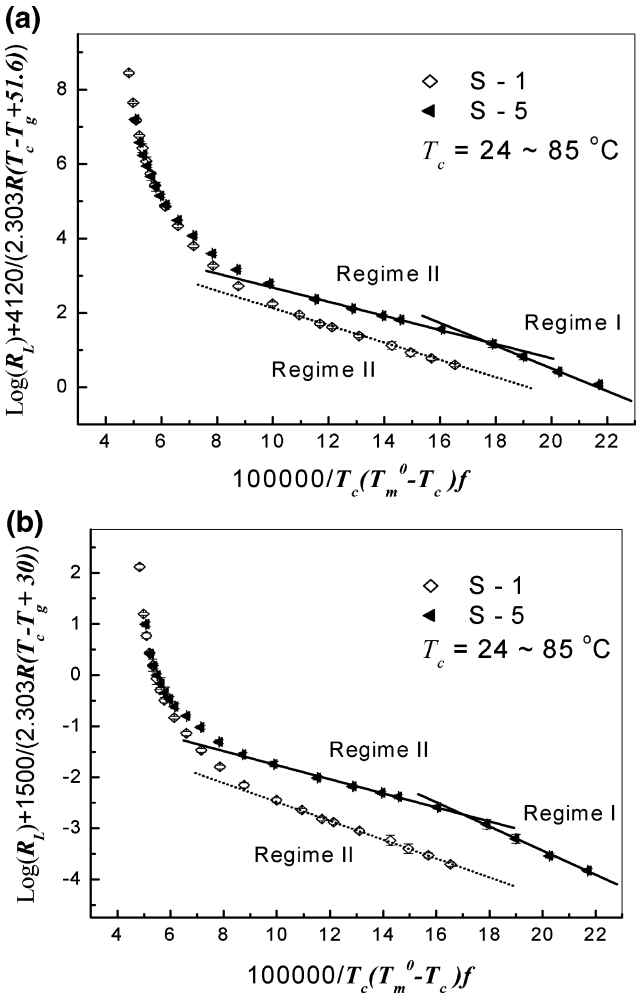

Figure 4. Plots of log $R_L + U^*/2.303R(T_c - T_\infty)$ vs $1/T_c(T_m^0 - T_c)f$ of BA-C8 samples (S-1 and S-5) in the temperature range from 24 to 85 °C: (a) the values of U^* and T_∞ are 4120 cal mol^{-1} and $T_\infty = T_g - 51.6$ °C, respectively; (b) the values of U^* and T_∞ are 1500 cal mol^{-1} and $T_\infty = T_g - 30$ K, respectively. The error bars represent standard deviations.

weight sample. Stiochiometric imbalances of 1.08, 1.085, 1.09, 1.10, 1.12, 1.14, and 1.16 were used and corresponded to BA-C8 samples S-1, S-2, S-3, S-4, S-5, S-6, and S-7, respectively. The MWs of the samples were determined by gel permeation chromatography at room temperature with tetrahydrofuran as the solvent.

The number-average molecular weight ($\bar{M}_n$), the weight-average molecular weight ($\bar{M}_w$), the polydispersity index ($\bar{M}_w/\bar{M}_n$), the T_g

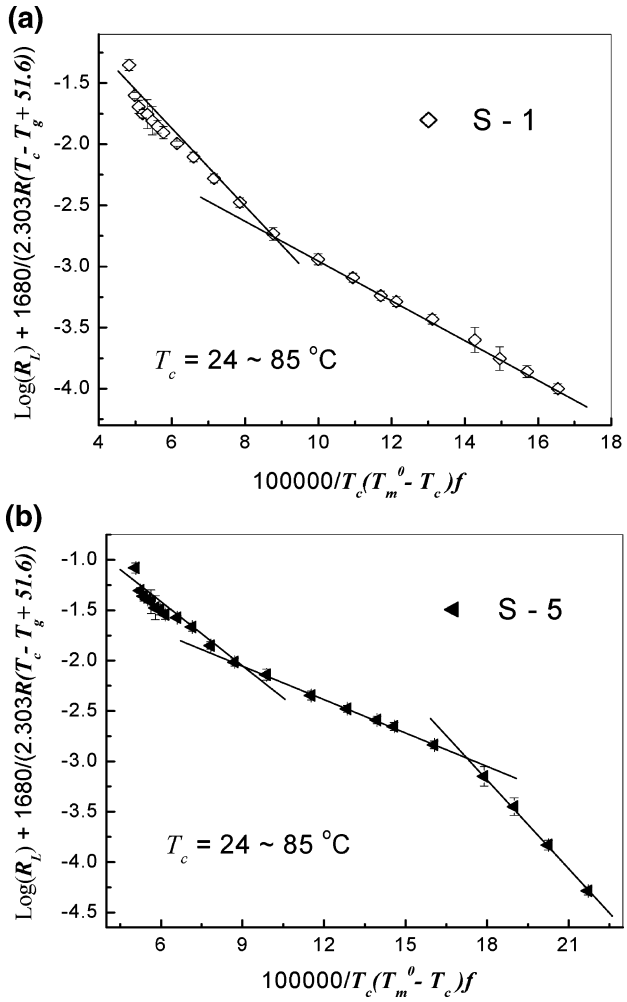

Figure 5. Two plots of log $R_L + U^*/2.303R(T_c - T_\infty)$ vs $1/T_c(T_m^0 - T_c)f$ of BA-C8 samples, (a) S-1 and (b) S-5, in the temperature range from 24 to 85 °C. The value of U^* is decreased to 1680 cal mol^{-1} in order to make the ratio of the slope values (K_{gIII}/K_{gII}) of the fitting lines of S-1 and S-5 be about 2. The error bars represent standard deviations.

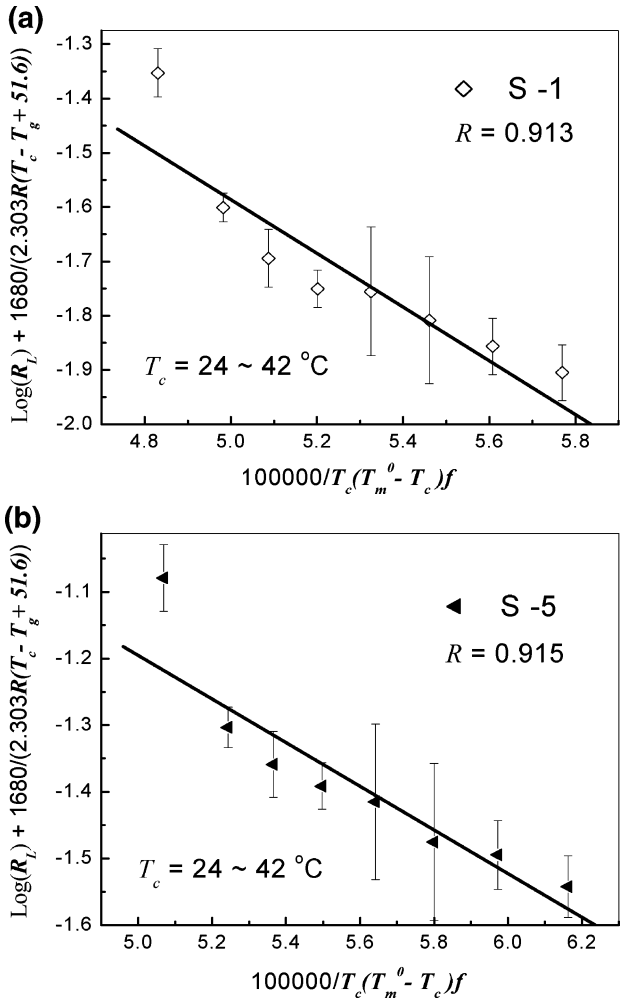

Figure 6. Two plots of log $R_L + U^*/2.303R(T_c - T_\infty)$ vs $1/T_c(T_m^0 - T_c)f$ of BA-C8 samples, corresponding to Figure 5, (a) S-1 and (b) S-5, respectively, in the temperature range from 24 to 42 °C. The R of the fitting lines in (a) S-1 and (b) S-5 are 0.913 and 0.915, respectively. The error bars represent one standard deviation.

and the T_m^0 of the BA-C8 samples are listed in Table 1. The T_m^0s of the samples were calculated using the Hoffman−Weeks method.[36] Figure 1 shows the plot of the melting point of sample S-3 as a function of the T_c. The T_m^0 was determined as the intersection between the plot for T_m vs T_c and the plot for $T_m = T_c$. It is well-known that the T_g of polymers is a function of molecular weight.[37,38] A plot of T_g as a function of $\bar{M}_n$ of the BA-C8 samples is given in Figure 2. The smallest value of $\bar{M}_n$, 6900 g/mol, is believed to be higher than the critical entanglement number-average molecular weight, $\bar{M}_c$ (labeled by b in Figure 2), which was estimated to be about 6000 g/mol. This value was estimated using the same number of skeletal bonds as the linear PE sample having an $\bar{M}_n$ of about 3800 g/mol, which is the $\bar{M}_c$ for PE. The choice of samples with an $\bar{M}_n$ above 6000 g/mol is to ensure that entanglements between polymer chains exist and that they increase as $\bar{M}_n$ increases. The maximum growth rate should occur at a temperature near $(T_g + T_m^0)/2$, which was calculated to be between 55 and 65 °C.

Thin films for AFM observations were prepared by spin-coating a 30 mg mL^{-1} polymer−chloroform solution onto silicon wafers (approximately 10 mm × 10 mm) at 3000 rpm. The samples were dried in a vacuum oven at room temperature for 15 min before AFM observations. The thickness of the amorphous polymer films was estimated to be ~300 nm using an ellipsometer. Tapping mode AFM images were obtained using a NanoScope III MultiMode AFM (Digital Instruments) equipped with a high-temperature heater accessory (Digital Instruments). Both topographic and phase images were recorded simultaneously using the retrace signal. Si tips (TESP) with a resonance frequency of ~300 kHz and a spring constant of about 40 N m^{-1} were used, and the scan rate was in the range of 0.4−1.2 Hz with the scanning density of 512 lines/frame. The set-point amplitude ratio, r_{sp} ($r_{sp} = A_{sp}/A_0$, where A_{sp} is the set-point amplitude and A_0 is the amplitude of the free oscillation, which was always 2.0 V in this study), was adjusted to be as large as possible, ranging from 0.7 to 0.9, to maintain a good balance between the quality of the images and the effects on lamellar growth and crystal morphology.

3. Results and Discussion

Dependence of the Lamellar Growth Rate on Temperature. The LH theory has been successfully used on many polymers to analyze growth rates (G) of spherulites or axialites. Three crystallization regimes have been confirmed in many melt crystallization studies of polymers.[6,39−43] Recently, the application of the LH theory has been extended to study the cold crystallization of polymers.[44−47] According to the LH theory, G is determined by the following equation:

$$G = G_0 \exp\left[-\frac{U^*}{R(T_c - T_\infty)}\right] \exp\left[-\frac{K_{g(i)}}{T_c(T_m^0 - T_c)f}\right] \quad (1)$$

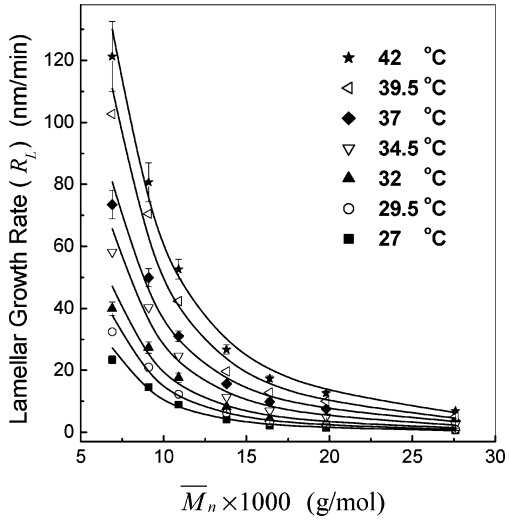

Figure 7. Plot of R_L vs $\bar{M}_n$ for various MW BA-C8 samples at various T_cs. The error bars represent one standard deviation.

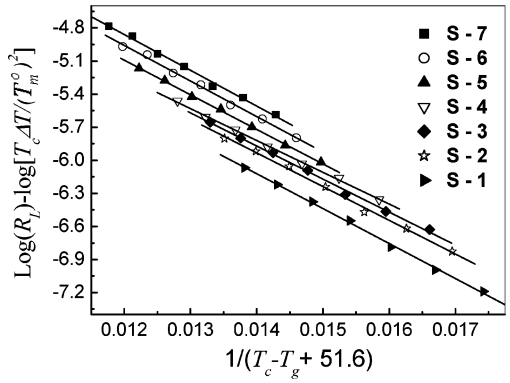

Figure 8. Plot of $\log R_L - \log[T_c\Delta T/(T_m^0)^2]$ vs $1/(T_c - T_g + 51.6)$ for various MW BA-C8 samples in the temperature range from 27 to 42 °C.

where G_0 is temperature insensitive but related to the MW of the polymer ($G_0 \propto MW^{\alpha}$), U^* is the activation energy for the transport process of a crystallizing unit from the liquid to the crystal surface, R is the gas constant, T_∞ is the temperature at which all segmental motions cease, $K_{g(i)}$ is the activation energy for the formation of a secondary nucleus of critical size in regime i, and f is a correction factor equal to $2T_c/(T_c + T_m^0)$.

The value of $K_{g(i)}$ can be determined from the slope of the plot of $\log G + U^*/2.303R(T_c - T_\infty)$ vs $1/T_c(T_m^0 - T_c)f$. According to the LH theory, the plot should exhibit two abrupt breaks as the crystallization temperature is lowered from a high value near the T_m^0 to a temperature near the T_g. The changes in the slope value indicate the changes in the kinetic mechanisms. These two breaks suggest that there are three regimes of crystal growth. The first regime (regime I), which is near the melting point of the polymer, captures a single nucleation per substrate length. In this regime, the nucleation rate is slower than the substrate completion rate. As the temperature decreases, the second regime (regime II) is reached when the nucleation rate equals or is greater than the substrate completion rate. A further decrease in temperature causes a rapid increase in the nucleation rate. In the final regime (regime III), the separation of niches on the substrate approaches the width of a single stem. The values of $K_{g(i)}$ in the three regimes is as follows: $K_{g(I)} = 2K_{g(II)} = K_{g(III)}$.

In this study, the crystallization of BA-C8 was studied at crystallization temperatures near the T_g of the polymer. Lamellar growth rates (R_L) instead of G were measured. The equivalence of $R_L$and G will be discussed in a forthcoming paper. During the crystallization study of the BA-C8 samples, an edge-on founding lamella that developed from a primary nucleus could be easily visualized by AFM. All other lamellae within the same spherulite (or crystal aggregate) were its descendants (subsidiary lamellae). The average growth rates of the founding lamellae and the subsidiary lamellae were calculated from the slope of the length of lamellae vs time. It is necessary to point out that each founding lamella has two growing tips, while a subsidiary lamella has only one. For convenience, we define the growth rate at one of the growing tips as the growth rate of the founding lamella. For each spherulite, one founding lamella and two subsidiary lamellae were chosen. Figure 3 shows the plots of a founding lamella and two subsidiary lamellae of sample S-5 as a function of time at 32 °C. The slope values of the founding lamella and two subsidiary lamellae are 34.2, 17.5, and 16.9 nm/min, respectively. Clearly, the average growth rates of all lamellae within a spherulite, including the founding lamella and subsidiary lamellae that grow outward radially on the fringe of a spherulite, are similar. In this study, 10 spherulites from each BA-C8 sample were used. Accordingly, the average growth rates of the lamellae, including the founding and subsidiary lamellae, of each BA-C8 sample, at a constant T_c were calculated using 30 slope values.

In order to understand the crystallization behavior of the BA-C8 system, the lamellar growth rates of samples S-1 and S-5 at temperatures ranging between T_g and T_m^0 were measured and subsequently analyzed using the LH theory. Here, two sets of values of U^* and T_∞ were used to obtain the best fit with the experimental data. One set of the values was $U^* = 4120$ cal mol^{-1} and $T_\infty = T_g - 51.6$ °C. The choice of $T_\infty = T_g - 51.6$ °C was used to describe the bulk viscous flow of the polymer between T_g and $T_g + 100$ °C according to the Williams−Landel−Ferry (WLF) theory.[20] The other values, which were $U^* = 1500$ cal mol^{-1} and $T_\infty = T_g - 30$ K, were obtained from the experimental measurements of many polymers at low temperatures.[48,49]

Figure 4a,b displays the plots of $\log R_L + U^*/2.303R(T_c - T_\infty)$ vs $1/T_c(T_m^0 - T_c)f$ of samples S-1 and S-5 in the temperature range from 24 to 85 °C. The values of $U^* = 4120$ cal mol^{-1} and $T_\infty = T_g - 51.6$ °C were used in Figure 4a, while $U^* = 1500$ cal mol^{-1} and $T_\infty = T_g - 30$ K were used in Figure 4b. It can be clearly seen that, using two different sets of values for U^* and T_∞, the shape of the plots is quite similar. There are three and two regions with a constant slope value in the plots of the S-5 sample (low MW, $\bar{M}_n = 10900$ g/mol) and S-1 sample (high MW, $\bar{M}_n = 27600$ g/mol), respectively. The slope ratios between regimes I and II of the S-5 sample determined from Figure 4a,b are about 1.78 and 2.33, respectively. These two slope ratio values are close to the theoretical value of 2, and the regime transition temperatures (between regimes I and II) displayed in Figure 4a,b for the S-5 sample are almost the same, indicating that the two sets of U^* and T_∞ did not significantly affect the determination of the regime transition temperature. The results, showing two crystallization regimes for S-1 and three regimes for S-5, are in line with the predictions of the LH theory, that the crystallization depends on the molecular weight (low MW samples have three regimes (I, II, and III) and high MW samples have two (II and III)). However, the determination of the transition temperature between regimes II and III is difficult. At low temperatures, the plots of $\log R_L + U^*/2.303R(T_c - T_\infty)$ vs $1/T_c(T_m^0 - T_c)f$ are not linear, as shown in Figure 4. Large values of $K_{g(III)}/K_{g(II)}$, which are often higher

than three and even reach to seven, were obtained in poly(butylene terephthalate) (PBT), poly(trimethylene terephthalate) (PTT), and PEEK.[42,45−47]

Modification of the input parameters, especially U^*, can effectively change the value of $K_{g(III)}/K_{g(II)}$ and the locations of the crystallization regimes. When using $U^* = 1680$ cal mol^{-1} and $T_\infty = T_g - 51.6$ °C, the ratios of the slope values ($K_{g(III)}/K_{g(II)}$) obtained from the plots for the S-1 and S-5 samples are 1.95 and 2.01, respectively, as shown in Figure 5a,b. Nevertheless, the data points did not follow a straight line in the temperature range of 24−42 °C. The correlation coefficients (R) of the fitting lines for the S-1 and S-5 samples are 0.913 and 0.915, respectively, as shown in Figure 6a,b. This deviation between experimental and theoretical results is too large to be acceptable.

Unlike crystallization at temperatures near T_m, in which the motion of polymer chains can be carried out entirely via molecular reptation, polymer chains complete their conformation rearrangement via cooperative segmental movements at crystallization temperatures near T_g. Indeed, the LH secondary nucleation theory was developed for highly crystallizable, flexible-chain polymers such as PE, assuming that chain folding following adjacent reentry occurred. However, the random reentry switchboard model seems to be better in describing crystallization of polymers at crystallization temperatures near T_g, especially polymers like BA-C8, which have semirigid chain structures, like PET and PEEK. The presence of bisphenol groups in the backbone of BA-C8 may make the adjacent reentry energetically unfavorable during crystallization at low temperatures.

Polymer crystallization is the transference of chains from the entangled disordered state to the ordered crystal state. At crystallization temperatures near T_g and with polymer chains attaching on a rough surface, secondary nucleation is assumed to be absent, and the crystallization process can be described as the continuous attachment and detachment of small chain segments on the crystal surface. The growth rate is determined by the balance between the rates of attachment and detachment.[50] In this model, all steps on the crystal surface are energetically identical and are accessible to all adjacent molecules. The attaching of a chain segment lowers the enthalpy. Half of the free energy of crystallization is assumed to be given to the activation energy of the attachment step, and the other half is given to the activation energy of the detachment step. The rates of attachment, r^+, and detachment, r^-, are determined from

$$r^+ = A\frac{kT_c}{h}\exp\left(-\frac{\Delta E - \epsilon/2}{kT_c}\right) = A\frac{kT_c}{h}\exp\left(-\frac{\Delta E}{kT_c}\right)\exp\left(\frac{\epsilon}{2kT_c}\right) \quad (2)$$

and

$$r^- = A\frac{kT_c}{h}\exp\left(-\frac{\Delta E}{kT_c}\right)\exp\left(-\frac{\epsilon}{2kT_c}\right) \quad (3)$$

respectively, where A is a temperature-insensitive prefactor, related to the chain-length-dependent kinetic process (i.e., A is regarded as a function of MW, $A \propto MW^\alpha$), such as entanglement or disentanglement of crystallizing chains and diffusion of crystallization units via cooperative segmental movements before and after chain depositing on the crystal surface; kT_c/h is the rate of thermal vibration; k is Boltzmann's constant; h is Planck's constant; ΔE is the activation energy for the chain transport of one segment; and ϵ is the decrease in the free energy upon attachment of a chain segment. As a result, the net rate of chain accretion, r, is expressed as

$$r = r^+ - r^- = A\frac{kT_c}{h}\exp\left(-\frac{\Delta E}{kT_c}\right)\left[\exp\left(\frac{\epsilon}{2kT_c}\right) - \exp\left(-\frac{\epsilon}{2kT_c}\right)\right] \quad (4)$$

It is reasonable to assume that $\epsilon \ll kT_c$ because only a small single chain segment is attached to the crystal growing surface. When $\epsilon \ll kT_c$, eq 4 can be rewritten as

$$r = r^+ - r^- = \frac{A}{h}\exp\left(-\frac{\Delta E}{kT_c}\right)\epsilon \quad (5)$$

The rate of a single lamellar growth rate, R_L, is related to r, as shown in the following equation:

$$R_L \propto r \propto B\exp\left(-\frac{\Delta E}{kT_c}\right)\epsilon \quad (6)$$

where $B = A/h$. The free energy difference (ϵ) between a chain segment in the amorphous phase adjacent to the crystal surface and the chain segment adsorbed onto the crystal surface is assumed to be related to the free energy difference between the amorphous phase and the crystal: $\epsilon \propto \Delta G$.

According to Hoffman,[51] for large degrees of supercooling, the ΔG at T_c is

$$\Delta G = \frac{T_c \Delta h \Delta T}{(T_m^0)^2} \quad (7)$$

where Δh is the heat of fusion. Combining eqs 6 and 7 yields

$$R_L \propto B\exp\left(-\frac{\Delta E}{kT_c}\right)\frac{T_c \Delta h \Delta T}{(T_m^0)^2} \quad (8)$$

From the WLF expression for viscous flow, the term $\exp(-\Delta E/kT_c)$ can be rewritten as[52]

$$\exp\left(-\frac{\Delta E}{kT_c}\right) = \exp\left[-\frac{C_1}{R(C_2 + T_c - T_g)}\right] \quad (9)$$

where $C_1 = 4120$ cal/mol, $C_2 = 51.6$ °C, and R is the gas constant. Substituting eq 9 into eq 8 gives

$$R_L \propto B\exp\left(-\frac{C_1}{R(T_c - T_g + 51.6)}\right)\frac{T_c \Delta T}{(T_m^0)^2} \quad (10)$$

It should be noted that the prefactor, B, in eq 10 should be similar to that in eq 2 and is related to the molecular weight of the polymer (i.e., $B \propto D\bar{M}_n^\alpha$, where D is a constant and α is the power parameter). Thus, taking the logarithm on both sides of eq 10 gives

$$\log R_L = \log D + \alpha\bar{M}_n - \frac{C_1}{2.303R(T_c - T_g + 51.6)} + \log\left(\frac{T_c \Delta T}{(T_m^0)^2}\right) \quad (11)$$

Figure 7 displays the plots of R_L vs $\bar{M}_n$ for BA-C8 samples at various T_cs, namely, 27, 29.5, 32, 34.5, 37, 39.5, and 42 °C. It can be clearly seen that R_L decreases sharply with increasing

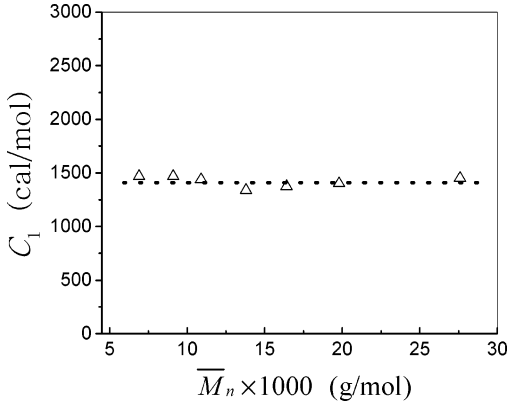

Figure 9. Plot of the calculated values of C_1 vs $\bar{M}_n$ for various MW BA-C8 samples.

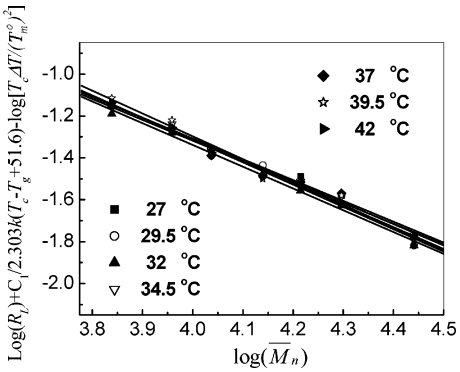

Figure 10. Plot of $\log R_L + C_1/2.303k(T_c - T_g + 51.6) - \log[T_c\Delta T/(T_m^0)^2]$ vs $\log(\bar{M}_n)$ of various MW BA-C8 samples used in the temperature range from 27 to 42 °C.

MW at any T_c. This result is in agreement with the theoretical prediction[1] and the published experimental data.[2] Figure 8 displays the plot of $\log R_L - \log[T_c\Delta T/(T_m^0)^2]$ vs $1/(T_c - T_g + 51.6)$ of BA-C8 samples with varied MW in the temperature range from 27 to 42 °C. The experimental data points follow straight lines with R larger than 0.995, confirming that eq 10, developed on the basis of the rough surface, is valid.

In addition, the values of C_1 that were determined from the slopes of the straight lines ranged from 1339 to 1469 cal/mol and did not vary much with the MW, as shown in Figure 9. It is generally accepted that, before crystallization takes place, polymer chains are always entangled with each other when $\bar{M}_n$ is larger the $\bar{M}_c$. Hence, the density of chain entanglements in BA-C8 films must increase with an increase in MW because all BA-C8 samples have larger $\bar{M}_n$ than the estimated $\bar{M}_c$. However, different degrees of chain entanglement in the BA-C8 films with varied MWs result in similar values for C_1, as shown in Figure 9. This result implies that there is no center-of-mass reptation of the chains but rather there is short-range motion of the chain segments on to the crystal growing surface during BA-C8 crystallization at temperatures near T_g; otherwise, C_1 should increase with MW.

The dependence of the lamellar growth rate on MW at temperatures near T_g was analyzed as a function of a power law, $R_L \propto \bar{M}_n^{\alpha}$, as given in eq 9, using $C_1 = 1426$ cal/mol. Figure 10 shows a plot of $\log R_L + C_1/[2.303k(T_c - T_g + 51.6)] - \log[T_c\Delta T/(T_m^0)^2]$ vs $\log(\bar{M}_n)$ in the temperature range from 27 to 42 °C. It can be easily seen that the slope values of every line at various temperatures are quite similar, as all slope values are in the range -1.0 to -1.1. This result reveals quite similar (or even the same) values of α for the power law, $R_L \propto \bar{M}_n^{\alpha}$, for crystallization of BA-C8 samples at temperatures near T_g.

4. Conclusion

At low crystallization temperatures, the effect of MW on the lamellar growth kinetics was investigated by AFM. The results of our analysis of the lamellar growth rates indicate that the LH theory cannot be used to describe the crystallization of BA-C8 polymers in regime III. A new expression of lamellar growth kinetics was proposed on the basis of a simple kinetic model of rough growth surfaces. This expression has been successfully used in analyzing the kinetic data obtained in regime III.

Acknowledgment. We are grateful for the support of the Hong Kong Government Research Grants Council under Grants 600503 and 600405.

References and Notes

(1) Hoffman, J. D.; Miller, R. L. *Macromolecules* **1988**, *21*, 3038.
(2) Magill, J. H. *J. Appl. Phys.* **1964**, *35*, 3249.
(3) Magill, J. H. *J. Polym. Sci.* **1967**, *A-2*, 89.
(4) Magill, J. H. *J. Polym. Sci.* **1969**, *A-2*, 1187.
(5) Hoffman, J. D. *Polymer* **1982**, *235*, 656.
(6) Cheng, S. Z. D.; Janimak, J. J.; Zhang, A. *Macromolecules* **1990**, *23*, 298.
(7) Lovering, E. G. *J. Polym. Sci.* **1970**, *C30*, 329.
(8) Godovsky, Y. K.; Slonimsky, G. L.; Garbar, N. M. *J. Polym. Sci.* **1972**, *C38*, 1.
(9) Chen, H. L.; Li, L. J.; Ouyang, W. C.; Hwang, J. C.; Wong, W. Y. *Macromolecules* **1997**, *30*, 1718.
(10) Umemoto, S.; Kobayashi, N.; Okui, N. *J. Macromol. Sci., Phys.* **2002**, *B41*, 923.
(11) Magill, J. H.; Kojima, M.; Li, H. M. IUPAC Symp. Macromol., Aberdeen, Sept 1973 (Abstract B-33).
(12) Nishi, M.; Hikosaka, M.; Toda, A.; Takahashi, M. *Polymer* **1998**, *39*, 1591.
(13) Okada, M.; Nishi, M.; Takahashi, M.; Matsuda, H.; Toda, A.; Hikosaka, M. *Polymer* **1998**, *39*, 4535.
(14) Hoffman, J. D.; Miller, R. L. *Polymer* **1997**, *38*, 3151.
(15) Sadler, D. M.; Gilmer, G. H. *Polymer* **1984**, *25*, 1446.
(16) Sadler, D. M. *Polymer* **1983**, *24*, 1401.
(17) Sadler, D. M. *J. Chem. Phys.* **1987**, *87*, 1771.
(18) Sadler, D. M. *Polymer* **1987**, *28*, 1440.
(19) De Gennes, P. G. *J. Chem. Phys.* **1971**, *55*, 572.
(20) Ferry, J. D. *Viscoelastic Properties of Polymers*, 3rd ed.; John Wiley & Sons: New York, 1980.
(21) Magonov, S. N.; Elings, V.; Whangbo, M. H. *Surf. Sci.* **1997**, *375*, L385.
(22) Pearce, R.; Vansco, G. J. *Macromolecules* **1997**, *30*, 5843.
(23) Hobbs, J. K.; Mcmaster, T. J.; Miles, M. J.; Barham, P. J. *Polymer* **1998**, *39*, 2437.
(24) Schultz, J. M.; Miles, M. J. *J. Polym. Sci., Polym. Phys.* **1998**, *36*, 2311.
(25) Li, L.; Chan, C. M.; Li, J. X.; Ng, K. M.; Yeung, K. L.; Weng, L. T. *Macromolecules* **1999**, *32*, 8240.
(26) Godovsky, Y. K.; Magonov, S. N. *Langmuir* **2000**, *16*, 3549.
(27) Jiang, Y.; Gu, Q.; Li, L.; Shen, D. Y.; Jin, X. G.; Lei, Y. G.; Chan, C. M. *Polymer* **2002**, *43*, 5615.
(28) Lei, Y. G.; Chan, C. M.; Li, J. X.; Ng, K. M.; Wang, Y.; Jiang, Y.; Li, L. *Macromolecules* **2002**, *35*, 6751.
(29) Hobbs, J. K.; Mamaster, J. J.; Miles, M. J.; Barham, P. J. *Polymer* **1998**, *39*, 2437.
(30) Li, L.; Chan, C. M.; Yeung, K. L; Li, J. X.; Ng, K. M.; Lei, Y. G. *Macromolecules* **2001**, *34*, 316.
(31) Hobbs, J. K.; Miles, M. J. *Macromolecules* **2001**, *34*, 353.
(32) Beekmans, L. G. M.; Vancso, G. J. *Polymer* **2000**, *41*, 8975.
(33) Lei, Y. G.; Chan, C. M.; Wang, Y.; Ng, K. M.; Jiang, Y.; Li, L. *Polymer* **2003**, *44*, 4673.
(34) Wang, Y.; Chan, C. M.; Ng, K. M.; Jiang, Y.; Li, L. *Langmuir* **2004**, *20*, 8220.
(35) Jiang, Y.; Yan, D. D.; Gao, X.; Han, C. C.; Jin, X. G.; Li, L.; Wang, Y.; Chan, C. M. *Macromolecules* **2003**, *36*, 3652.
(36) Hoffman, J. D.; Week, J. J. *J. Chem. Phys.* **1965**, *42*, 4301.
(37) Fox, T. G.; Flory, P. J. *J. Appl. Phys.* **1950**, *21*, 581.
(38) Fox, T. G.; Flory, P. J. *J. Polym. Sci.* **1954**, *14*, 315.
(39) Hoffman, J. D. *Polymer* **1983**, *24*, 3.
(40) Phillips, P. J.; Vatansever, N. *Macromolecules* **1987**, *20*, 2138.

(41) Clark, E. J.; Hoffman, J. D. *Macromolecules* **1984**, *17*, 878.
(42) Runt, J.; Miley, D. M.; Zhang, X.; Gallagher, K. P.; McFeaters, K.; Fishburn, J. *Macromolecules* **1992**, *25*, 1929.
(43) Hong, P.-D.; Chung, W.-T.; Hsu, C.-F. *Polymer* **2002**, *43*, 3335.
(44) Lu, H. B.; Nutt, S. *J. Appl. Polym. Sci.* **2003**, *89*, 3464.
(45) Qiu, Z. B.; Mo, Z. S.; Zhang, H. F.; Sheng, S. R.; Song, C. S. *J. Polym. Sci.: Part B: Polym. Phys.* **2000**, *38*, 1992.
(46) Liu, T. X.; Mo, Z. S.; Wang, S. E.; Zhang, H. F. *Eur. Polym. J.* **1997**, *33*, 1405.
(47) Medallin-Rodroguez, F. J.; Phillips Lin, J. S. *Macromolecules* **1995**, *28*, 7744.
(48) Suzuki, T.; Kovacs, A. *Polym. J.* **1970**, *1*, 182.
(49) Lauritzen, J. I., Jr.; Hoffman, J. D. *J. Appl. Phys.* **1973**, *44*, 4340.
(50) Schultz, J. M. *Polymer Crystallization: The Development of Crystalline Order in Thermoplastic Polymers*; American Chemical Society: Washington, DC, 2001.
(51) Hoffman, J. D. *J. Chem. Phys.* **1958**, *29*, 1192.
(52) Boon, J.; Azcue, J. M. *J. Polym. Sci., Part A2* **1968**, *6*, 885.

MA062717Y